Uluslararası İleri Doğa Bilimleri ve Mühendislik Araştırmaları Dergisi
Sayı 9, S. 270-276, 12, 2025

Araştırma Makalesi

International Journal of Advanced Natural Sciences and Engineering Researches
Volume 9, pp. 270-276, 12, 2025

Research Article

https://as-proceeding.com/index.php/ijanser
ISSN:2980-0811

UV-Vis-NIR Photodetector Produced Using *Lavandula angustifolia* Extract: A Green Approach

Mehmet Hakan ÇOLPAN[1,2]

[1]*Deparment of Property Protectıon and Securıty, Kadınhanı Faik İçil Vocational School, Selcuk University, 42800, Konya, Türkiye*

[2]*Department of Biotechnology, Faculty of Science, Selcuk University, 42130 Konya, Türkiye*

hakan.colpan@selcuk.edu.tr

(Received: 02 December 2025, Accepted: 07 December 2025)

(5th International Conference on Recent Academic Studies ICRAS 2025, December 02-03, 2025)

ATIF/REFERENCE: Çolpan, M. H. (2025). UV-Vis-NIR Photodetector Produced Using Lavandula angustifolia Extract: A Green Approach, *International Journal of Advanced Natural Sciences and Engineering Researches*, 9(12), 270-276.

Abstract-In this study, the usability of *Lavandula angustifolia* (lavender), a natural plant extract, as an active material in the production of photodetectors was investigated. An environmentally friendly and self-powered photodetector capable of broad-band detection in the UV-Vis-NIR (ultraviolet-visible-near infrared) spectral range was successfully produced with a simple and low-cost method. The basic performance parameters of the photodetector, namely photosensitivity (I_{ph}), photosensitivity (K), responsivity (R) and specific detectability (D*), were investigated in detail at different wavelengths. The obtained data show that the device exhibits high performance especially in the range of 351–1000 nm and reaches maximum values at 1000 nm ($I_{ph}=1.58\times10^{-5}$ A, R=0.1 A/W, D*=1.82×10^{10} Jones). Significant decreases were observed in these parameters at wavelengths above 1000 nm. These results demonstrate that lavender extract-based natural material offers a promising photodetector platform for applications from UV to near-infrared.

Keywords: Supercritical CO_2 Extraction, Schottky Photodiode, Lavandula angustifolia, Photodetector.

I. INTRODUCTION

Photodetectors play a vital role in optoelectronic systems by converting light into electrical signals and are widely used in fields like optical communication, environmental monitoring, and biomedical imaging [1–3]. Their performance depends on charge carrier dynamics—mainly electrons and holes—generated through processes such as thermal excitation, photo-generation, and impact ionization [4,5]. A key structure in many photodetectors is the metal–semiconductor (MS) junction, which forms a Schottky barrier when a metal like platinum or tungsten interfaces with semiconductors like silicon or gallium arsenide, significantly affecting device behavior [6].

In recent years, the rapid development of nanotechnology has significantly advanced the field of optoelectronics [7]. Semiconductors, as core materials in these devices, have drawn considerable attention due to their tunable optical and electronic characteristics [8]. Photodetectors that operate in the UV and visible regions—often based on pn junctions with bandgaps tailored to specific wavelengths—are widely explored for use in applications like space communication, night vision, missile detection, and bio/chemical sensing [9].

Effective photodetection depends on the alignment between the photon energy and the bandgap of the semiconductor material. Wide bandgap semiconductors are required for UV detection. Although silicon is a commonly used semiconductor, its relatively narrow bandgap limits its responsiveness across broad spectral ranges, especially in the UV and IR regions [10,11]. Additionally, most traditional photodetectors require external biasing to separate photo-generated carriers, which raises concerns related to power consumption and device complexity. This has led to growing interest in self-powered photodetectors that can function without an external power source [12,13].

Extensive research has been conducted on innovative photodetector designs. For example, Vashishtha et al. (2025) reported a self-biased multilayer photodetector based on MoS_2–Sb_2Se_3–GaN, capable of detecting a broad spectral range from UV-C to IR-B, achieving a responsivity of 665 mA/W and detectivity of 4.19×10^{10} Jones under UV-A light [14]. In another study, they developed a near-infrared photodetector using nano-fenced MoS_2, offering high sensitivity and thermal stability [15]. They also introduced an f-TiO_2/GaN photodetector with exceptionally high responsivity (~34,000 A/W) and external quantum efficiency (~1.2×10^7%) [16]. More recently, organic photodetectors (OPDs) have emerged as promising alternatives due to their advantages such as flexibility, solution-processability, and tunable optoelectronic properties [17]. One notable direction involves the use of plant-based materials as interlayers. Yıldırım et al. (2024), for instance, developed a UV-vis-IR OPD using Epilobium angustifolium extract, achieving a responsivity of 0.65 A/W and detectivity of 1.41×10^{12} Jones under IR light [18]. Özer et al. (2025) fabricated a UV-A photodiode with *Stachys lavandulifolia* extract, reporting a responsivity of 0.109 A/W and detectivity of 9.39×10^{11} Jones [19]. Other notable works include Abd and Mohi's (2023) silver oxide-based photodetector enhanced with Anemone coronaria dye, which showed improved infrared response [20]; Thu et al.'s (2018) study on tomato-derived films for UV detection [21]; and Latief et al.'s (2023) use of Borago officinalis extract in a ZnO-based photodetector, achieving detectivity of 1.3×10^{13} and EQE of 119% at 950 nm [22]. Yuca et al. (2023) developed a hybrid UV/IR photodetector combining *Hibiscus sabdariffa* extract with n-Si, showing excellent rectification and broadband photoresponse [23]. Doğan et al. (2024) demonstrated a self-powered photodetector using curcumin and n-Si, achieving a detectivity of 1.22×10^{11} Jones and responsivity of 13.19 A/W under 395 nm UV light at -2 V [24].

In the present study, *Lavandula angustifolia* extract was utilized as an organic interlayer, obtained through supercritical CO_2 extraction. A hybrid photodetector was fabricated by combining this extract with an n-type silicon substrate. The device's electronic and optoelectronic properties were systematically evaluated under UV, visible, and near-infrared illumination.

II. MATERIAL METHOD

Lavandula angustifolia were sourced from the campus of Selçuk University in Konya, Turkey, and dried naturally at ambient temperature. The extraction process was carried out using a SUPEREX F-500 supercritical CO_2 extractor, operating at 40 °C and 250 bar. The extraction lasted for 90 minutes, after which the obtained extract was stored at −20 °C until further use.

Phosphorus-doped n-type silicon (n-Si) substrates with a resistivity range of 1–20 Ω·cm and thickness between 500–550 µm were procured from Wafer World. These wafers were diced into 15 × 15 mm² segments and cleaned using the standard RCA ultrasonic method [25]. Ohmic contacts were formed on the back side of the n-Si wafers by depositing aluminum via physical PVD. A solution of *Lavandula angustifolia* extract (20 mg/mL in ethanol) was then spin-coated onto the front surface of the n-type Si at 2000 rpm for 30 seconds. The resulting films were subjected to mild heating (~50 °C) to remove residual solvent. Subsequently, aluminum top contacts were deposited on the coated surface using PVD. The fabricated device had an active area of 7.85×10^{-3} cm². Electrical and optoelectronic measurements were conducted using a Keithley 2400 Sourcemeter and a Fytronix 7000 solar simulator. For spectral response testing, visible light filters (351–1600 nm) from Thorlabs GmbH, Germany, were employed.

III. THE RESEARCH FINDINGS AND DISCUSSION

The electrical behavior of the Schottky diodes was evaluated through current–voltage (I–V) measurements. Upon illumination, photocurrent generation in photodiodes can occur via three main mechanisms: (1) electron excitation and transfer from the metal to the semiconductor; (2) generation of electron–hole pairs within the depletion region; and (3) avalanche multiplication under high reverse bias. The observed changes in reverse current with applied voltage are largely attributed to the photoexcitation of charge carriers from the valence band into defect-related energy levels within the material. The increase in reverse current with higher light intensities clearly indicates the photodiodes' sensitivity to illumination and is consistent with typical photodetection behavior [26].

The logarithmic (LnI–V) curves of the *Lavandula angustifolia*/n-Si device are presented in Figure 1. Measurements were taken under different wavelengths and compared with those obtained under dark conditions. Under forward bias, the device exhibited only a slight increase in current. Upon illumination, the incoming light generates photocarriers, facilitating charge transport and enabling current flow. This behavior highlights the diode's sensitivity to light and its potential for optoelectronic applications.

The key performance parameters defining the behavior of a photodetector include photocurrent (I_p), photosensitivity (K), responsivity (R), and detectivity (D*). These parameters are calculated using the following equations:

$$I_p = I_{light} - I_{dark} \tag{1}$$

$$K = \frac{I_p}{I_{dark}} \tag{2}$$

$$R = \frac{I_p}{PA} \tag{3}$$

$$D^* = \frac{\sqrt{S}}{NEP} \tag{4}$$

Here, A represents the active area of the detector, P is the incident light power density, e is the elementary charge, I_{dark} is the dark current, and S is the detector area. D* quantifies the detector's ability to detect weak signals relative to noise. Responsivity (R) is defined as the ratio of electrical output to optical input. Photosensitivity (K) quantitatively describes the relative increase in current due to light exposure. Specific detectivity (D*) characterizes the detector's ability to detect weak optical signals amid noise.

In Figure 2a, the photocurrent (I_{ph}) values remain relatively constant across the UV to near-infrared range (351–1000 nm), peaking at 1000 nm and then sharply declining, indicating a significant reduction in photoresponse in the mid-infrared region. Figure 2b shows a similar trend for responsivity, where R steadily increases, reaching a peak of 0.1 A/W at 1000 nm, and then decreases significantly beyond this point. In Figure 2c, photosensitivity (K) closely follows the trends of Iph and R, maintaining high values up to 1000 nm before declining, suggesting reduced efficiency in converting light into electrical signals at longer wavelengths.

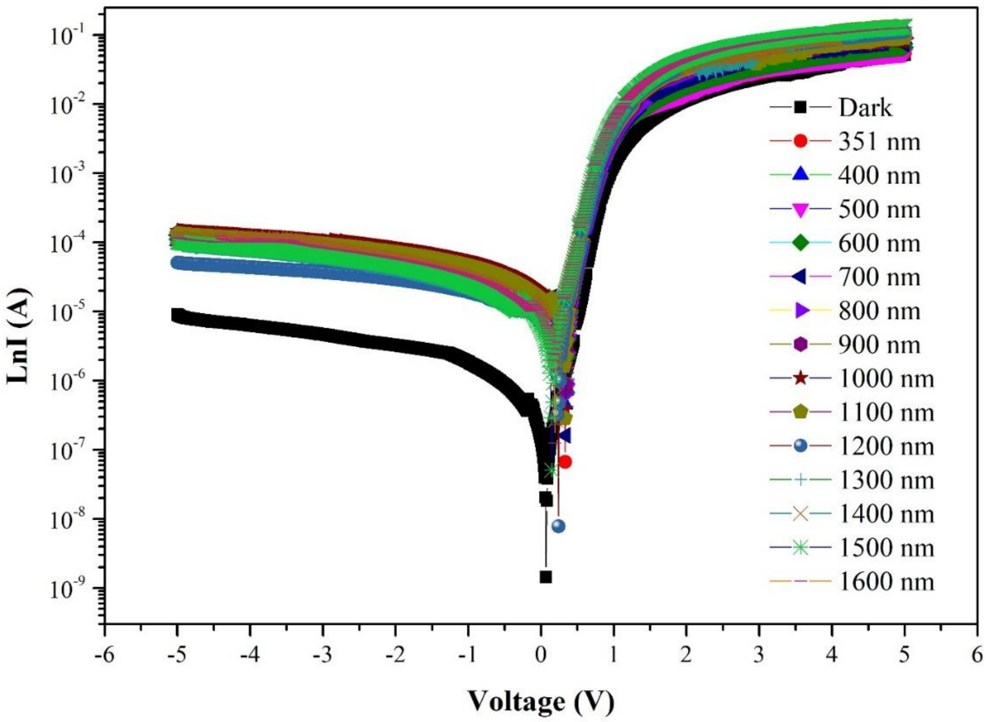

Figure 1. LnI–V curves of the Lavandula angustifolia/n-Si device under different wavelengths

Finally, Figure 2d displays the detectivity, which peaks at approximately 1000 nm (1.82×10^{10} Jones), highlighting optimal signal-to-noise performance in this spectral range. Beyond 1000 nm, D* significantly decreases, reflecting a reduction in detection capability due to increased noise and diminished responsivity. These graphs collectively confirm that the photodetector operates most efficiently in the UV to near-infrared spectrum and is less suitable for mid-infrared applications.

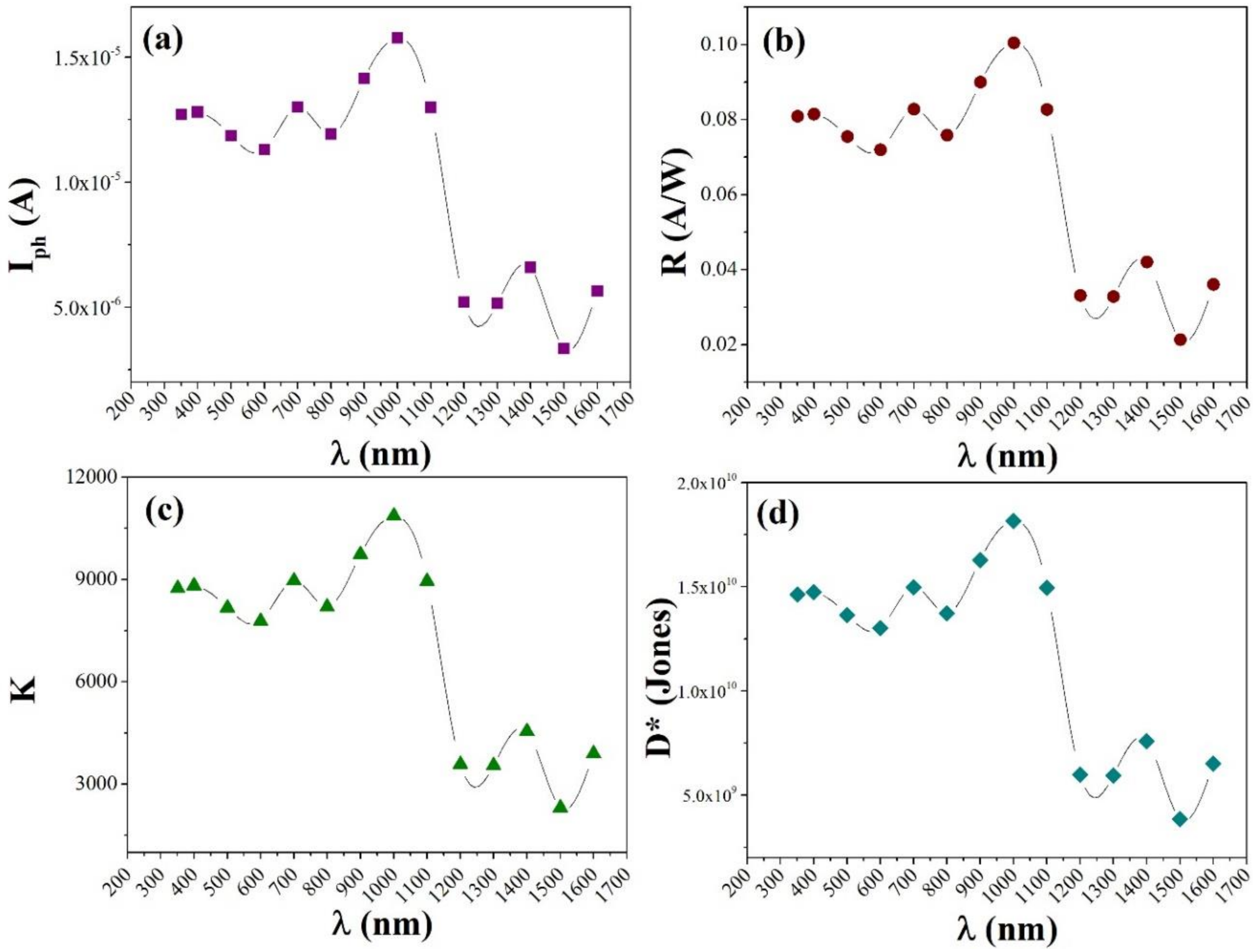

Figure 2. (a) Iph–λ, (b) R–λ, (c) K–λ, and (d) D–λ curves*

Table 1 presents the spectral performance analysis of the *Lavandula angustifolia*/n-Si photodetector across wavelengths ranging from 351 nm to 1600 nm. Key measured parameters include photocurrent (I_{ph}), photosensitivity (K), responsivity (R), and detectivity (D*). The device shows high performance in the UV to near-infrared range (351–1000 nm), evidenced by higher photocurrent values (peaking at 1.58×10^{-5} A at 1000 nm), maximum photosensitivity (up to 10,860), and relatively high responsivity (up to 0.1 A/W). Specific detectivity also reaches its maximum at 1000 nm (1.82×10^{10} Jones), indicating optimal sensitivity to weak signals in this region.

However, beyond 1000 nm, all performance metrics exhibit a notable decline. For example, responsivity drops to 0.021 A/W at 1500 nm, and D* decreases to 3.86×10^{9} Jones. This suggests a reduction in detection efficiency in the mid-infrared region. This analysis reveals that the photodetector is most suitable for applications involving wavelengths between UV and near-infrared.

Table 1. Photodetector parameters

λ (nm)	I_{ph} (A)	K	R (A/W)	D* (Jones)
351	1.27×10^{-5}	8744	0.081	1.46×10^{10}
400	1.28×10^{-5}	8814	0.081	1.47×10^{10}
500	1.19×10^{-5}	8164	0.075	1.37×10^{10}
600	1.13×10^{-5}	7783	0.072	1.30×10^{10}
700	1.30×10^{-5}	8958	0.083	1.50×10^{10}
800	1.19×10^{-5}	8204	0.076	1.37×10^{10}
900	1.41×10^{-5}	9735	0.090	1.63×10^{10}
1000	1.58×10^{-5}	10860	0.100	1.82×10^{10}
1100	1.30×10^{-5}	8947	0.083	1.50×10^{10}
1200	5.20×10^{-6}	3584	0.033	5.99×10^{9}
1300	5.15×10^{-6}	3550	0.033	5.94×10^{9}
1400	6.60×10^{-6}	4543	0.042	7.60×10^{9}
1500	3.35×10^{-6}	2306	0.021	3.86×10^{9}
1600	5.66×10^{-6}	3896	0.036	6.51×10^{9}

IV. RESULTS

In this study, *Lavandula angustifolia* extract was obtained using the supercritical CO_2 extraction method, and an environmentally friendly, sustainable, and low-cost photodetector was developed using this natural material. The supercritical CO_2 method is an extraction technique that leaves no solvent residue and can isolate target components with high purity, thereby enhancing the suitability of the extract for photonic applications. The resulting photodetector demonstrated high performance in the UV-Vis-NIR spectral range, particularly between 351–1000 nm, highlighting the potential of plant-based materials for optoelectronic applications.

The photodetector exhibited strong broadband performance across 351–1600 nm, with optimal response in the visible to near-infrared range (351–1100 nm). Peak photocurrent (1.58×10^{-5} A), responsivity (0.100 A/W), photosensitivity (10,860), and detectivity (1.82×10^{10} Jones) were recorded at 1000 nm, demonstrating high efficiency and signal clarity. Although a gradual decline in performance was observed beyond 1200 nm, the device maintained detectable response up to 1600 nm, confirming its capability for wide-spectrum applications.

The device achieved its maximum value for photocurrent, photosensitivity, responsivity, and detectivity at 1000 nm, indicating this region as optimal for photodetection. Although a decline in performance was observed at wavelengths beyond 1000 nm, this approach presents an effective alternative for sustainable technologies. In the future, structurally modifying such natural-source materials could lead to devices capable of detecting across a broader spectrum.

CONFLICTS OF INTEREST
No conflict of interest was declared by the authors.

REFERENCES

[1] Q. Lin, A. Armin, P. L. Burn, and P. Meredith, “Filterless narrowband visible photodetectors,” *Nat. Photonics*, 9(10):687–694, (2015).

[2] Q. Li, Y. Guo, and Y. Liu, “Exploration of Near-Infrared Organic Photodetectors,” *Chem. Mater.*, 31(17):6359–6379, (2019).

[3] H. Ren, J. Chen, Y. Li, and J. Tang, “Recent Progress in Organic Photodetectors and their Applications,” *Adv. Sci.*, 8 (1), (2021).

[4] D. A. Neamen and D. Biswas, *Semiconductor Physics and Devices : Basic Principles*. New York: McGraw-Hill higher education, (2011).

[5] V. K. S. Hsiao *et al.*, “Photo-carrier extraction by triboelectricity for carrier transport layer-free photodetectors,” *Nano Energy*, 65:103958, (2019).

[6] T. Akila, P. Gayathri, G. Alan Sibu, V. Balasubramani, H. Al-Lohedan, and D. M. Al-Dhayan, “Augmented photovoltaic performance of Cu/Ce-(Sn:Cd)/n-Si Schottky barrier diode utilizing dual-doped Ce-(Sn:Cd) thin films,” *Opt. Mater. (Amst).*, 149:115133, (2024).

[7] K. Kasthuri, J. K. Kumar, P. Rajkumar, S. Kalpana, and V. Balasubramani, “Feasible antibacterial nanomaterials: Copper oxide nanoparticles synthesized using dandelion leaf extract,” *Inorg. Chem. Commun.*, 167:112804, (2024).

[8] G. Alan Sibu, P. Gayathri, T. Akila, R. Marnadu, and V. Balasubramani, “Manifestation on the choice of a suitable combination of MIS for proficient Schottky diodes for optoelectronic applications: A comprehensive review,” *Nano Energy*, 125:109534, (2024).

[9] S. Pan, Q. Liu, J. Zhao, and G. Li, “Ultrahigh Detectivity and Wide Dynamic Range Ultraviolet Photodetectors Based on Bi x Sn 1– x O 2 Intermediate Band Semiconductor,” *ACS Appl. Mater. Interfaces*, 9(34):28737–28742, (2017).

[10] Z. Li, T. Yan, and X. Fang, “Low-dimensional wide-bandgap semiconductors for UV photodetectors,” *Nat. Rev. Mater.*, 8(9):587–603, (2023).

[11] S. Li, Y. Zhang, W. Yang, H. Liu, and X. Fang, “2D Perovskite Sr2Nb3O 10 for High-Performance UV Photodetectors,” *Adv. Mater.*, 32(7), (2020).

[12] F. Yıldırım, S. Khalili, Z. Orhan, H. M. Chenari, and Ş. Aydoğan, “Highly sensitive self-powered UV-visible photodetector based on ZrO2-RGO nanofibers/n-Si heterojunction,” *J. Alloys Compd.*, 935:168054, (2023).

[13] D. Periyanagounder, P. Gnanasekar, P. Varadhan, J.-H. He, and J. Kulandaivel, “High performance, self-powered photodetectors based on a graphene/silicon Schottky junction diode,” *J. Mater. Chem. C*, 6(35):9545–9551, (2018).

[14] P. Vashishtha, A. Dash, S. Walia, and G. Gupta, “Self-bias Mo–Sb–Ga multilayer photodetector encompassing ultra-broad spectral response from UV–C to IR–B,” *Opt. Laser Technol.*, 181:111705, (2025).

[15] P. Vashishtha, P. Prajapat, A. Sharma, P. Goswami, S. Walia, and G. Gupta, “Self-driven and thermally resilient highly responsive nano-fenced MoS2 based photodetector for near-infrared optical signal,” *Mater. Res. Bull.*, 164:112260, (2023).

[16] P. Vashishtha *et al.*, “Strong light-matter interaction and antireflection functionality of f-TiO_2/GaN heterostructure broadband photodetector,” *J. Alloys Compd.*, 948:169735, (2023).

[17] X. Zhang, J. Jiang, B. Feng, H. Song, and L. Shen, “Organic photodetectors: materials, device, and challenges,” *J. Mater. Chem. C*, 11(37):12453–12465, (2023).

[18] F. Yıldırım, S. Karakaya, H. Yuca, Ü. İncekara, and Ş. Aydoğan, “Self-powered high-performance UV–vis–IR hybrid photovoltaic photodetector based on Epilobium angustifolium L. (Onagraceae),” *J. Alloys Compd.*, 979:173584, (2024).

[19] S. Özer, Ö. Sevgili, Y. Yapar, and İ. Orak, “The plant-based photodiode with Stachys lavandulifolia interfacial layer,” *Sensors Actuators A Phys.*, 382:116122, (2025).

[20] A. N. Abd and A. T. Mohi, “Effect of Plant Extract Anemone Coronaria Concentration on the Spectral Response of the AgO / PSi Photodetector Effect of Plant Extract Anemone Coronaria Concentration on the Spectral Response of the AgO / PSi Photodetector,” *ACE J. Adv. Res. Phys. Sci.*, 1:5–11, (2023).

[21] M. M. Thu, A. Mastuda, and K. Y. Cheong, “Effects of drying temperature on tomato-based thin film as self-powered UV photodetector,” *Appl. Surf. Sci.*, 445:186–196, (2018).

[22] E. A. Latief, A. T. Mohi, and A. N. Abd, “Effect of Natural Dye on the Spectral Response of the Heterojunction Ag/ZnO/Ps/Si/Ag for Photodetector Application,” *Int. J. Nanosci.*, 22(6), (2023).

[23] H. Yuca, S. Karakaya, F. Yıldırım, Ü. İncekara, and Ş. Aydoğan, “Highly responsive self-driven broadband hybrid photodetector with high detectivity and on/off ratio based on Hibiscus sabdariffa,” *Phys. Scr.*, 98(12):125982, (2023).

[24] H. O. Dogan, F. Yıldırım, Z. Orhan, A. Ben Ahmed, M. Benhaliliba, and Ş. Aydoğan, “Numerical evaluations of curcumin organic molecule and an experimental study on hybrid photodetector performance in visible and UV regions,” *Org. Electron.*, 124:106946, (2024).

[25] W. Kern and D. A. Puotinen, “Cleaning Solutions Based on Hydrogen Peroxide for Use in Silicon Semiconductor Technology,” *RCA Rev.*, 31:187–206, (1970).

[26] H. Aydin, A. Tataroğlu, A. A. Al-Ghamdi, F. Yakuphanoglu, F. El-Tantawy, and W. A. Farooq, “A novel type heterojunction photodiodes formed junctions of Au/LiZnSnO and LiZnSnO/p-Si in series,” *J. Alloys Compd.*, 625:18–25, (2015).